GROUNDWATER GEOCHEMISTRY AND ASSOCIATED HARDPANS IN SOUTHWESTERN AUSTRALIA

Sam Lee

CRC LEME, Department of Applied Geology, Curtin University of Technology, Bentley, Western Australia, 6485

INTRODUCTION

The mineralogy and geochemistry of pedogenic and groundwater silcretes and ferricretes and associated groundwater geochemistry were investigated for deeply weathered, highly kaolinised regolith in southwestern Australia. The silcretes and ferricretes form shallow hardpans and impede drainage of the highly saline, acidic, shallow groundwaters in lower valleys of the subdued, ancient landscape. These valleys are associated with discharge of groundwater and the formation of saline seeps, which hosts a variety secondary minerals including amorphous silica [opal-CT], goethite [α-FeOOH], hematite [α-Fe2O3], akaganeite [ß-FeOOH], jarosite [KFe3(SO4)2(OH)6], barite [BaSO4], gypsum [CaSO4.2H2O], and halite [NaCl].

RESULTS AND DISCUSSION

The shallow hardpans underlying the saline seeps contain abundant silicified and ferruginised pseudomorphs of plant roots and indicate that biogeochemical processes were involved in the removal of groundwater and concentration of silicon and iron. Silicified roots are commonly present in silcrete with remarkable preservation of cellular structures by almost pure SiO_2 (Figure 1, Table 1). The presence of silcrete lenses at great depths may indicate that deep root systems (e.g., eucalyptus species) have penetrated to a water table much lower than present day levels or that subsequent sedimentation has buried there lenses. The former is likely due to the evidence of a possible root channel between depths of 20-30 metres in the silicified granite pallid zone.

The silcretes and ferricretes also occur as vertical sequences of near parallel, discontinuous layers in the regolith (Thiry & Milnes 1991). Silica and iron oxyhydroxide minerals indurated diverse regolith including colluvium and alluvium consisting of heterogeneous mixtures of clay and rounded to angular grains of quartz and feldspars derived from the erosion of mostly granitic pallid and saprolite zones and fragments of lateritic materials. The iron oxide minerals in these cements include Al-goethite and Al-hematite, which occur as void fillings and/or are diffused through the silica indurated kaolin matrix.
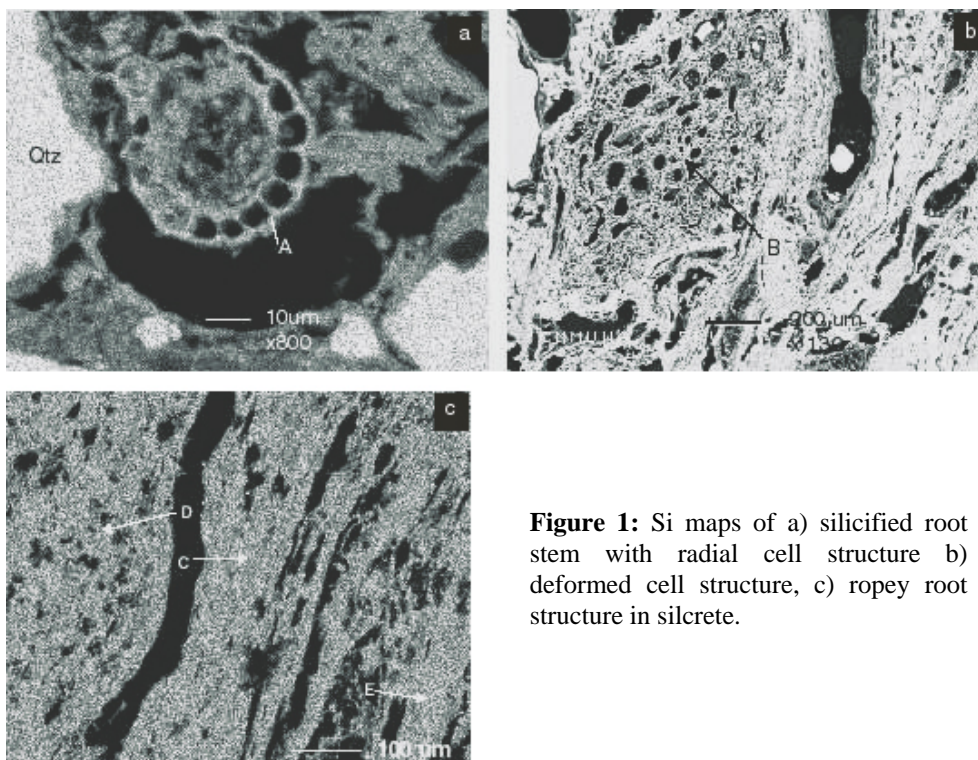

Figure 1: Si maps of a) silicified root stem with radial cell structure b) deformed cell structure, c) ropey root structure in silcrete.

Table 1: Spot EMPA analysis of points from Figure 1.

Spot	SiO_2	Al_2O_3	Fe_2O_3	Al_2O_3/SiO_2
A	83.36	12.88	2.3	0.15
B	99.58	0.00	0.00	0.00
C	97.83	1.25	0.48	0.01
D	99.53	0.23	0.00	0.00
E	99.56	0.18	0.26	0.00
F	99.79	0.12	0.00	0.00
Mean	96.61	2.44	0.51	0.03

Deep groundwater silcretes are composed of silicified *in situ* lateritic pallid zone materials and saprolite that have developed from granitic rocks (Butt 1985). The matrix consists of amorphous silica diffused through a porous kaolin groundmass (Singh 1992). These materials were initially highly porous but the voids are now occupied by amorphous silica and secondary anatase (Figure 2). Acid groundwater weathering has resulted in the dissolution of most primary silicates including feldspars and micas (Figure 3 and 4), which has greatly elevated the concentration of dissolved silicon in groundwaters. Isovolumetric weathering of feldspar produced highly porous assemblages of fine-grained kaolin and minor halloysite, which can contain high concentrations of amorphous silica (up to about 50%) occupying these pores (Singh 1992). Alkali feldspars alter to kaolin pseudomorphs that are much more porous than vermicular kaolin pseudomorphs replacing mica, consequently these pseudomorphs contain much less amorphous silica (Singh 1991).
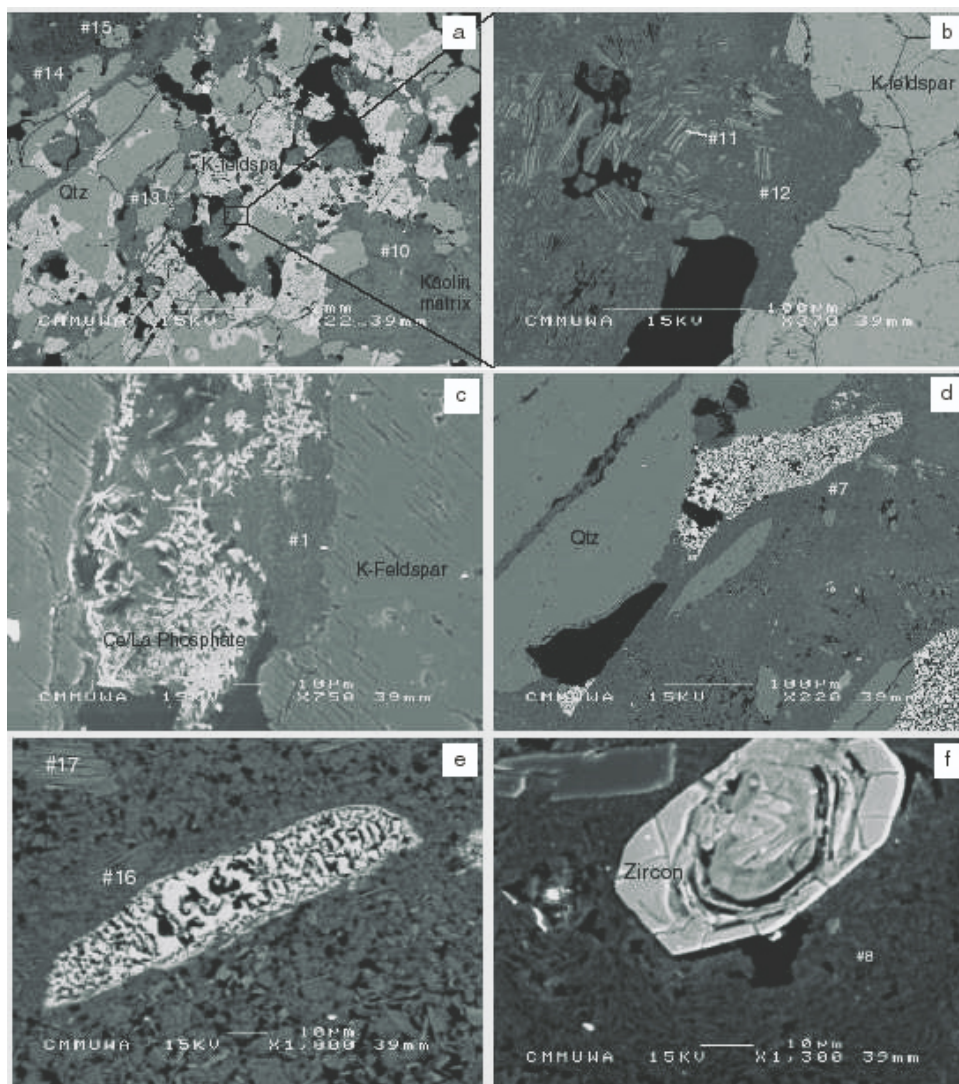

Figure 2: Back scattered (SEM) images of type II silcrete showing (a) quartz-feldspar framework and silica indurated kaolin matrix (b) enlarged area of matrix showing vermicular altered muscovite and kaolin (c) void filling of needle-shaped cerium/lanthanum phosphate in the intra-granular boundaries between primary K-feldspar grains and (d)-(e) replacement texture of secondary anatase in voids, (f) sub-euhedral to euhedral zircon with growth zones preserved.

The quantification of amorphous silica in the fine-grained kaolin matrix was achieved by using Al_2O_3/SiO_2

ratios obtained from SEM electron microprobe analyses. This procedure enabled mapping of the distribution of amorphous silica in silcrete at a micrometre scale. The recognition of abundant amorphous silica was supported by observation of a broad opal-CT XRD band centered at approximately 4Å and a brown, isotropic matrix observed from optical microscopy.
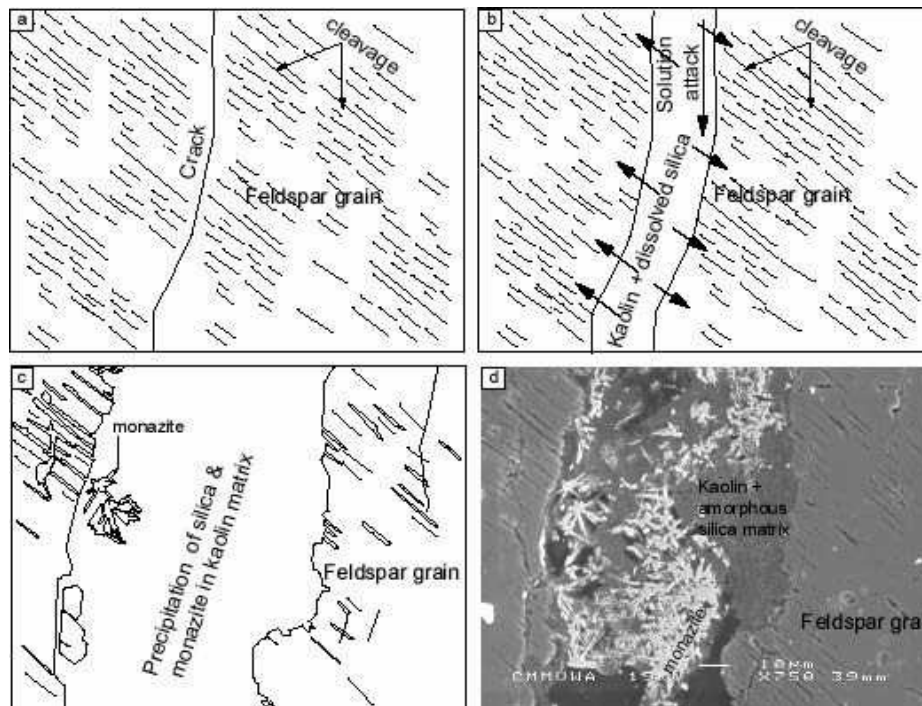

Figure 3: Illustration of (a) primary feldspar showing lamella structure, cleavage and cracks, (b) solution attack along cracks and dissolution of grain edges, (c) precipitation of secondary monazite and silica in the voids in the kaolin matrix that has partly replaced the parent feldspar, (d) back scattered electron (SEM) micrographs of groundwater silcrete at Merredin corresponding to the illustrations.
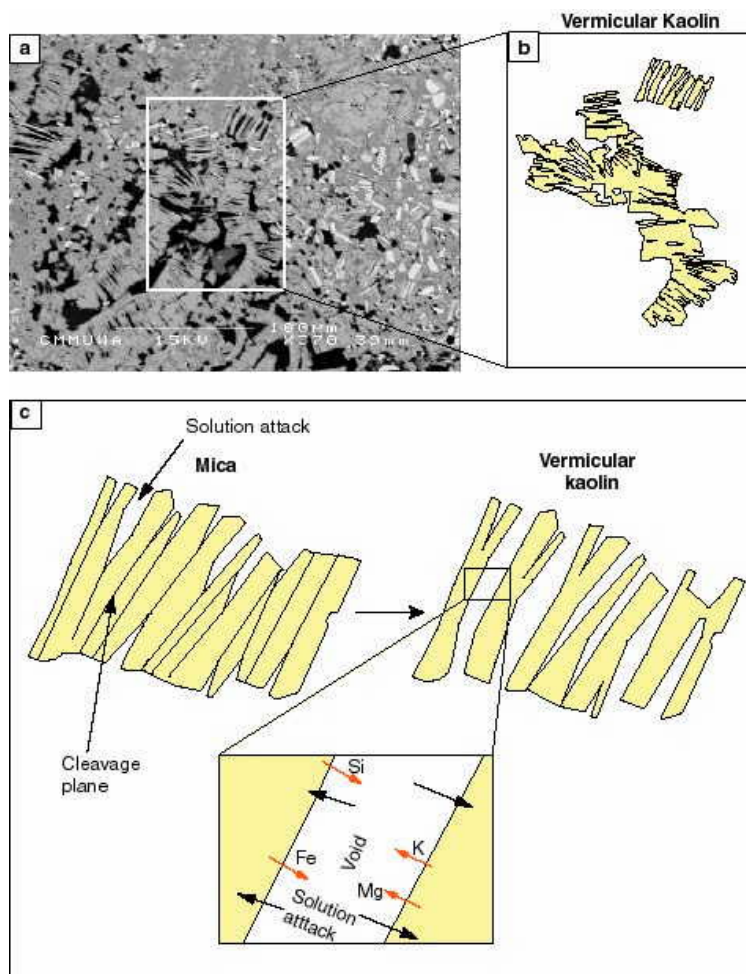

Figure 4: Illustration of the alteration of mica crystal (a) Back scattered electron (SEM) micrograph of Yalanbee groundwater silcrete showing (b) vermicular kaolin form (c) topotactic alteration of mica (e.g. biotite) by cation exchange with dissolution of basal faces within cleavages.

When dissolved silicon data for all field sets are combined, the homogeneous cluster of data points in the dissolved silicon vs. pH diagram (Figure 5a) is divided into a group of clusters when silicon is plotted against EC (Figure 5b). Multiple regression of EC and pH on dissolved silicon concentrations showed that most of the variation in silicon can be explained by pH and EC. In Figure 5b, two distinct trends can be seen. The lower pH and less saline groundwaters (between 2.8 to 3.99) contain higher concentrations of dissolved silicon than the relatively higher pH and more saline groundwater (pH 6 to 7.18). This association may imply that both pH and EC control the concentration of silicon in groundwater.
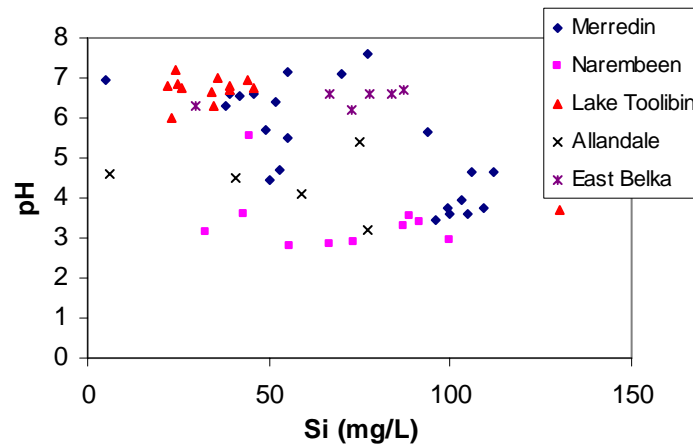

Figure 5a: Relationship between pH and dissolved silicon for all groundwaters in catchments. Note: Most of Merredin, Lake Toolibin, Allandale and East Belka groundwaters follow the negative trend.
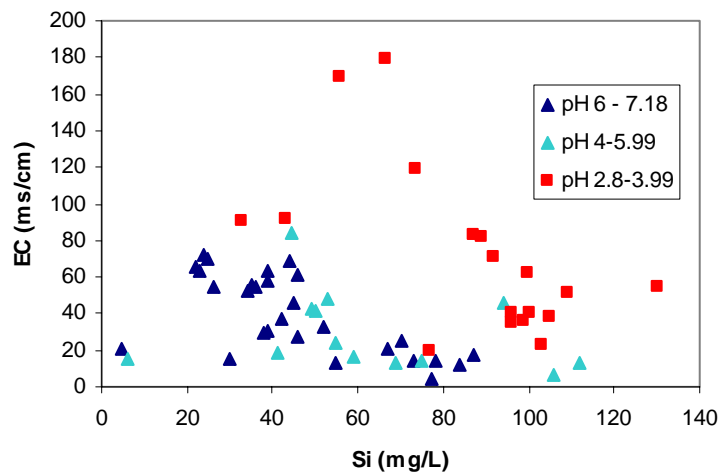

Figure 5b: Relationship between salinity (EC), dissolved silicon and pH.

Geochemical modelling using PHREEQC (Parkhurst & Appelo 1999) enabled prediction of the saturation state of minerals and indicated the dissolution and precipitation reactions occurring in the regolith-groundwater environment. Acid, moderately saline groundwaters were in near equilibrium with respect to amorphous silica, while near neutral pH, saline groundwaters corresponded to undersaturated conditions (Figure 6). For extremely acid groundwaters (pH<3.5), PHREEQC predicted dissolution of kaolin, goethite and hematite, which is reflected in the elevated concentrations of iron (up to 169 mg/L) and aluminium (up to 389 mg/L) in the groundwater.

SUMMARY

Silcrete in regolith consisting of diverse kaolin-quartz materials indurated by opal-CT is of common occurrence in southwest Australia. The occurrence of this material is related to the acid, Si-rich groundwaters that pervade regolith in this region. The opaline silica fills micrometric voids between kaolin crystals and may have replaced kaolin to some extent but this is not proven. Water use by plants is likely to be

responsible for the formation of continuous and discontinuous lenticular bodies of silcrete. The presence of subsurface silcrete has major influences on hydrogeology, plant growth and development of salinity.
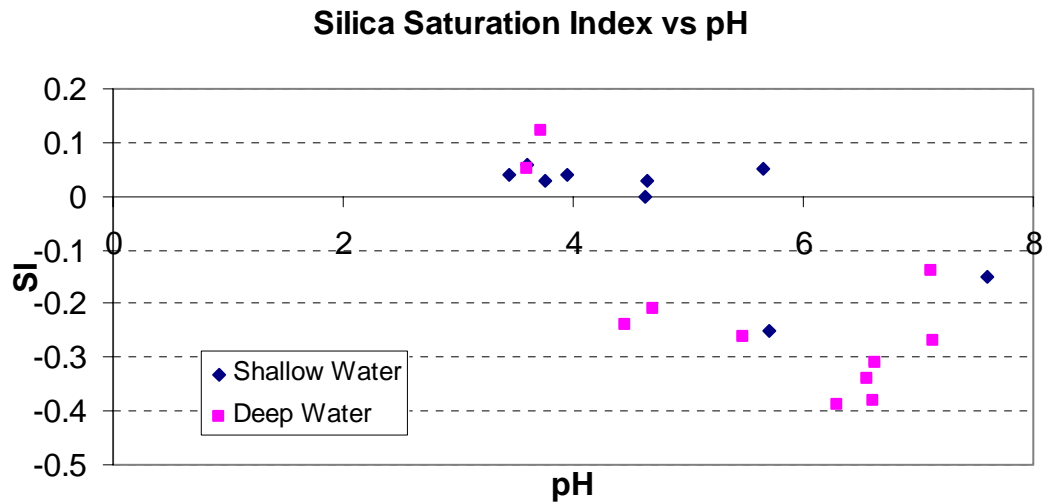
Silica Saturation Index vs pH

Figure 6: Saturation with respect to amorphous silica predominantly occurs at low pH and for shallow groundwaters.

REFERENCES

BUTT C.R.M. 1985. Granite weathering and silcrete formation on the Yilgarn Block, Western Australia. *Australian Journal of Earth Sciences* **32(4)**, 415-432.

PARKHURST D.L. & APPELO C.A.J. 1999. *User's guide to PHREEQC (version 2)- a computer program for speciation, batch-reaction, one-dimensional transport, and inverse geochemical calculations.* Water Resources Investigation **Report 99-4259**, Denver, Colorado.

SINGH B. & GILKES R.J. 1991. Alteration of Cr-muscovite to kaolinite in a weathered quartzite. *Clays and Clay Minerals* **39**, 571-579.

SINGH B. 1992. *Application of electron optical techniques to studies of soil materials.* PhD Thesis, University of Western Australia.

THIRY M. & MILNES A.R. 1991. Pedogenic and groundwater silcretes at Stuart Creek Opal field, South Australia. *Journal of Sediment Petrology* **61(1)**, 111-127.